Current Harmonics Suppression of Permanent Magnet Synchronous Motor Based on Repetitive Control

Quntao An, Xingya Liu, Qi An, Shuai Li, Kaitao Bi
Department of Electrical Engineering
Harbin Institute of Technology
Harbin, China
anquntao@hit.edu.cn

ABSTRACT: **In permanent magnet synchronous motor (PMSM) drive systems, there are 5th, 7th, 11th, 13th and other low order current harmonics due to the non-ideal factors such as the distortion of the air-gap field and the nonlinear characteristics of the inverter. In order to suppress the current harmonics and improve the system performance, repetitive controller is employed in parallel with proportional integral (PI) controller of current loop in the synchronous rotating dq coordinate system in this paper. Repetitive control originates from the internal model principle of control theory, which has inhibitory effect on periodic disturbances. It can suppress integer harmonic of a given frequency and get high-accuracy output waveforms. This method does not need to increase any hardware, and is easy to implement. Simulations and experiments are carried out to verify the effectiveness of the proposed method for current harmonic suppression.**

Keywords—permanent magnet synchronous motor(PMSM); current harmonics; repetitive control; harmonic suppression

I. INTRODUCTION

Due to its advantages of small volume, high efficiency, high power density and high torque output ratio, permanent magnet synchronous motor (PMSM) has been widely applied in high-precision servo drive, electric vehicle, aerospace and daily life [1]. However, due to the machining process deviation of motor body structure, the nonlinear factors of inverter in the drive system and the accuracy of digital controller, there are a series of harmonic components in currents of PMSM, which bring many adverse effects to the performance of the motor. It mainly focuses on two aspects to suppress harmonic currents. One is to optimize the design of motor body and improve the sinusoidal of air gap magnetic field [2]. The other is to compensate the harmonic current produced by the nonlinear factors of the inverter, and to achieve the purpose of suppression [3].

In [4], PI controllers in multiple rotating coordinate systems are used to cancel harmonics in the current of the motor and suppress the electromagnetic torque ripple of the motor by extracting the harmonic current in real-time and injecting the harmonic voltage. However, the algorithm is so complicated. In [5], the current compound regulator of PI and PR in the synchronous rotating dq coordinate system is proposed to suppress the specified current harmonics by using the no-error tracking characteristic of the proportional resonance controller for the sinusoidal variables, and the current harmonics suppression is achieved. But when the resonant regulator is used for motor control, the output current will overshoot when the input signal is the step signal, which affects the high performance torque control [6]. While the suppression of inverter harmonic current in other literatures is usually suppressed by means of without dead time control mode [7] or time compensation [8]. However, the two methods have the problems that the current zero-crossing detection is inaccurate, which easily leads to the error compensation and poor applicability [9].

The basic idea of repetitive controller is derived from the internal model principle of control theory [10], which can suppress periodic disturbances. Therefore, it can inhibit the low-order harmonic current such as 5th, 7th, 11th, 13th harmonics. Considering the many factors of harmonic generation and the disadvantages of the above-mentioned methods of harmonic suppression, this paper presents a suppression method based on repetitive controller in parallel with traditional current PI regulator, which can improve motor sinusoidal current and reduce the torque ripple of the motor. Finally, effectiveness of the proposed method are verified by simulations and experiments.

II. HARMONIC MATHEMATICAL MODEL OF PMSM

Because of the deviation of the motor structure design, the cogging effect and the structural defects of the rotor permanent magnet, the distribution of the rotor permanent flux linkage in the air gap circle is non-sinusoidal, which will cause the back EMF waveform distortion of the motor and the harmonic components in the motor current. Most of the motors are symmetrical distribution of three phase windings and star connections, so the EMF waveform is half wave symmetry, that is, the back EMF waveform does not contain even times harmonics and the integer multiple harmonics of 3 times. In other words, the main harmonic contents are 5th and 7th harmonics.

978-1-5386-5782-9/18/$31.00 ©2018 IEEE.

Under the synchronous rotating coordinate system of d-q, the voltage equation of PMSM [11] is

$$\begin{cases} u_d = R_s i_d - \omega L_q i_q \\ u_q = R_s i_q + \omega L_d i_d + \omega \psi_f \end{cases} \quad (1)$$

And,the equation of torque is

$$T_e = \frac{3}{2} p[(L_d - L_q) i_d i_q + \psi_f i_q] \quad (2)$$

Where $u_{d(q)}$ is the *d(q)* axis voltage components, $i_{d(q)}$ is the *d(q)*axis current components, $L_{d(q)}$ is the *d(q)* axis inductance, ψ_f is the flux linkage , R_s is the stator resistance, ω is the angular electric velocity of fundamental voltage, and T_e is the electromagnetic torque of motor, respectively.

Because of the nonlinearity of the inverter, such as the dead time and the conduction pressure drop, the current harmonics will be caused. The principle diagram of phase *a* bridge arm of the power inverter is shown in Fig.1. Taking phase *a* as an example for analysis, waveforms of the dead time effect of the phase *a* when $i_a>0$ is shown in Fig. 2. The T_{dead} is the dead time, and the turn-on and turn-off time of the switch is set to T_{on} and T_{off}. The total switching time error of a switch in the leg *a* during a switching cycle is T_d, that is

$$T_d = T_{dead} + T_{on} - T_{off} \quad (3)$$

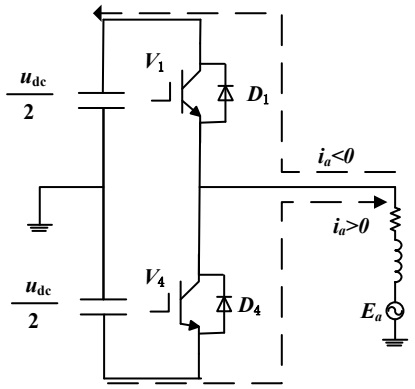

Fig.1. Phase *a* diagram of the inverter

In Fig. 2, S^*_1, S^*_2 is the ideal PWM signal for the upper and lower bridge arms. S_1 and S_2 are the corresponding actual PWM signals, u^*_a, u_a are the ideal and actual output voltages of the bridge arm.

In general, because of the dead time is added to the PWM signal, there is a voltage difference between the ideal output voltage of the inverter and the actual output voltage [12]. The voltage difference formula as follows:

$$u'_{err} = u_a - u^*_a \quad (4)$$

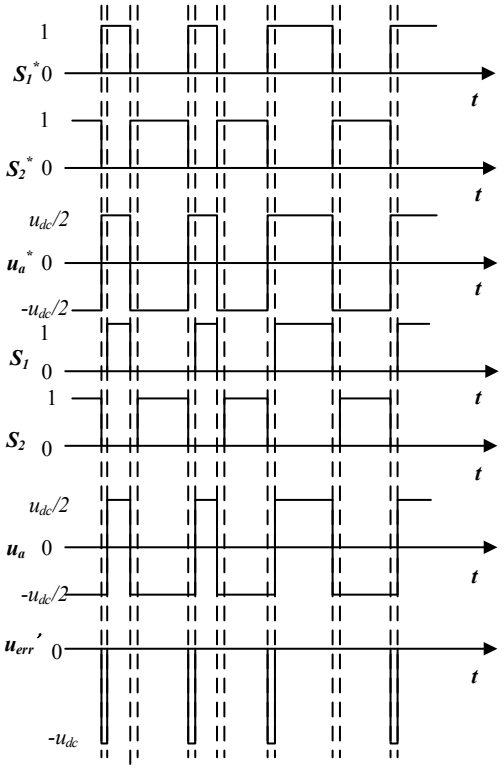

Fig. 2. The waveform of the dead time effect of phase *a* at $i_a>0$

In Fig. 2, it can be seen that output error voltage difference is a pulse voltage with negative amplitude, which is equal to the DC bus voltage, denoted by u_{dc}. The cycle of u_{dc} is also the period of PWM.

In addition to the dead time will lead to voltage waveform distortion, the inverter switching device IGBT conduction voltage drop, denoted by v_t, and diode freewheeling voltage drop, denoted by v_d, the output voltage waveform will also be distorted. Therefore, in the case of the tube pressure drop, the output voltage error waveform is shown in Fig. 3.

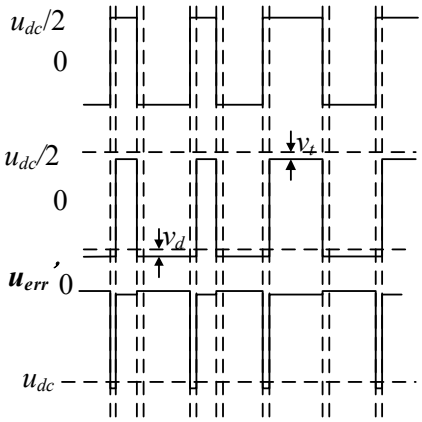

Fig.3. Voltage waveform of phase *a* at $i_a>0$

On the basis of the previous analysis, the PWM's cycle T_{pwm} is relatively small and assumes that $v_t=v_d$, so the error voltage of each cycle can be expressed equivalent. The size of

the average error voltage is denoted by Δu, when the A phase current is positive, error voltage as follows.

$$\Delta u = -\frac{T_d}{T_{pwm}}(u_{dc} + v_d - v_t) - \frac{v_d + v_t}{2} \tag{5}$$

In the same way, when the A phase current is negative:

$$\Delta u = \frac{T_d}{T_{pwm}}(u_{dc} + v_d - v_t) + \frac{v_d + v_t}{2} \tag{6}$$

The square wave signal of the error voltage is transformed by Fourier transform, available mathematical expression is:

$$u_{err} = \frac{4|\Delta u|}{\pi}(\cos\omega t + \frac{1}{3}\cos 3\omega t + \frac{1}{5}\cos 5\omega t + \frac{1}{7}\cos 7\omega t + \ldots \tag{7}$$

According to the results of Fourier decomposition, the nonlinear characteristics of inverter will lead to the distortion of output voltage waveform, and a large number of harmonics are introduced. On the one hand the PMSM mostly adopts star connection, the harmonic component of integer multiple of three times or three times will be offset. On the other hand , the higher the number of harmonics is, the smaller the amplitude is. So the number of harmonics introduced by the inverter is mainly 5 times and 7 times.

III. HARMONIC SUPPRESSION STRATEGY

A. Repetitive controller

The transfer function of the repetitive controller is as follows:

$$G(s) = \frac{e^{-sL}}{1 - e^{-sL}} \tag{8}$$

Here the L is the period of the given signal. But the pure delay link is difficult to use analog components, so the repetitive control is more used in discrete digital forms. Its discrete form is

$$G(z) = \frac{z^{-N}}{1 - z^{-N}} \tag{9}$$

Where N is a cycle of sampling times. The repetitive controller's internal model is similar to the integral part, but differs from the PI regulator in that it accumulates the error signal every N sample periods. The internal controller of repetitive controller is equivalent to an arbitrary signal generator, which has infinite gain for repetitive control frequency and multiple times. Therefore, repetitive control can completely suppress periodic disturbances.

The repetitive controller consists of a delay element and a positive feedback. As shown in Fig. 4 shows the general repetitive control system diagram, where *r* is the reference signal, *y* is the output signal, *e* is the error signal, *d* is the equivalent periodic disturbance, z^{-N} is the periodic delay, N is a fundamental period Of the sampling times, *C(z)* is the repetitive control loop compensator and *P(z)* is the control object.

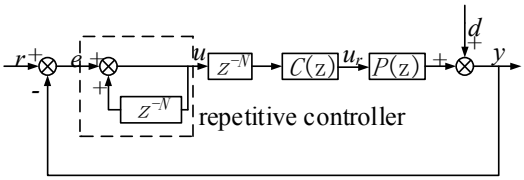

Fig.4. Diagram of repetitive control system

The introduction of repetitive controller inner mold will bring N poles on the unit circumference. The control theory shows that the system is in critical state and the stability of the system is poor, which is easy to make the system become unstable because of model error and disturbance factors. Therefore, it is generally necessary to improve internal mold to ensure that the system is stable and convergent. The current main method is to use Qz^{-N} instead of z^{-N}, and Q can be a constant less than 1 or a function with low - pass properties. Due to the introduction of Q, the improved internal model output cannot completely repeat the signal of the last cycle, but with a certain degree of attenuation. In this paper, Q is a constant less than 1, which can not only increase the stability of the system, but also do not change the form of the signal. When the inner mold is improved, the next analysis of its stability. In Fig.4, we can get the relationship between the output of the system and the input and disturbance as follows.

$$\begin{aligned} y(z) = &\frac{z^{-N}C(z)P(z)}{1 - z^{-N}(Q - C(z)P(z))}r(z) \\ &+ \frac{1 - Qz^{-N}}{1 - z^{-N}(Q - C(z)P(z))}d(z) \end{aligned} \tag{10}$$

The characteristic equation of the system is

$$1 - z^{-N}(Q - C(z)P(z)) = 0 \tag{11}$$

According to the control theory, it can be found that the stability of a discrete system can be solved by solving the characteristic equation. If the N solution of the characteristic equation is located in the unit circle of the z plane, it can be shown that the repetitive control system is stable. Theoretical analysis shows that if z_j is one of the solutions of the characteristic equation, then when the system is stable, there will be $|z_j| < 1$. At this time, $|z_j|^N < 1$ is inevitable. Therefore, for the characteristic equation, $|z_j^{-N}| = |Q - C(z_j)P(z_j)| < 1$ is established. In other words, only to meet $|Q - C(z)P(z)| < 1$, the system will be stable. Although the stability determination

method is simple, it is not the necessary condition for the stability of the system, but it is only sufficient condition.

B. Influence of internal mode factor Q on repetitive controller

After the constant coefficient Q is introduced into the repetitively controlled internal model, the repetitive control usually appears as a quasi-resonant at each resonance point. The derivation process is as follows:

The following formula is known from the math manual:

$$\pi \frac{e^{\pi x}+e^{-\pi x}}{e^{\pi x}-e^{-\pi x}} = x\sum_{k=-\infty}^{\infty}\frac{1}{x^2+k^2} \tag{12}$$

Equivalent deformation can be obtained:

$$\pi \frac{e^{\pi x}+e^{-\pi x}}{e^{\pi x}-e^{-\pi x}} = \frac{1}{\pi x}+\frac{2x}{\pi}\sum_{k=1}^{\infty}\frac{1}{x^2+k^2} \tag{13}$$

The internal mode form of the repetitive controller can be obtained:

$$G(s) = K\times\frac{e^{-sL}}{1-Qe^{-sL}} = K_{rc}\times\frac{Qe^{-sL}}{1-Qe^{-sL}} \tag{14}$$

Combination of (13), (14) can be obtained:

$$\begin{aligned} G(s) &= K_{rc}\times\frac{Qe^{-sL}}{1-Qe^{-sL}} = -\frac{K_{rc}}{2}+\frac{K_{rc}}{2}\frac{1+Qe^{-sL}}{1-Qe^{-sL}} \\ &= -\frac{K_{rc}}{2}+\frac{K_{rc}}{2}\frac{e^{\frac{1}{2}sL-C}+e^{-(\frac{1}{2}sL-C)}}{e^{\frac{1}{2}sL-C}-e^{-(\frac{1}{2}sL-C)}} \end{aligned} \tag{15}$$

Combination of (13), (15) can be obtained:

$$\begin{aligned} G(s) &= -\frac{K_{rc}}{2}+\frac{K_{rc}}{2}\frac{e^{\frac{1}{2}sL-C}+e^{-(\frac{1}{2}sL-C)}}{e^{\frac{1}{2}sL-C}-e^{-(\frac{1}{2}sL-C)}} = -\frac{K_{rc}}{2}+\frac{K_{rc}}{sL-2C} \\ &+\frac{2K_{rc}}{L}\sum_{k=1}^{\infty}\frac{s-\frac{2C}{L}}{s^2-2s\frac{2C}{L}+(\frac{2C}{L})^2+(\frac{2\pi k}{L})^2} \end{aligned} \tag{16}$$

Where $C=\frac{1}{2}\ln Q$, $\pi x=\frac{1}{2}sL-C$. Let $\omega_c=-\frac{\ln Q}{L}$ and substitute (16) can be obtained:

$$\begin{aligned} G(s) &= -\frac{K_{rc}}{2}+\frac{K_{rc}}{sL+\omega_c L}+\frac{2K_{rc}}{L}\sum_{k=1}^{\infty}\frac{s+\omega_c}{s^2+2s\omega_c+(\omega_c)^2+(\frac{2\pi k}{L})^2} \\ &\approx -\frac{K_{rc}}{2}+\frac{K_{rc}}{sL+\omega_c L}+\frac{2K_{rc}}{L}\sum_{k=1}^{\infty}\frac{s+\omega_c}{s^2+2s\omega_c+(k\omega)^2} \end{aligned} \tag{17}$$

The condition that the equal sign is equal to the number is that ω_c is much smaller than the fundamental frequency ω. Therefore, the mathematical relationship between the resonant bandwidth ω_c and the repetitive control internal model coefficient Q can be obtained from above. As indicated in (17), the repetitive controller with the constant Q added in the internal model is mainly composed of multiple quasi-resonant controllers with a resonant bandwidth of ω_c.

As shown in Fig.5, with the decrease of Q, the gain of the repetitive controller at the resonant frequency point is greatly reduced, and the bandwidth near the resonant frequency point is significantly increased. Therefore, the repetition control with a smaller internal mode coefficient reduces the sensitivity of the frequency fluctuation. However, the reduction of the internal mode factor causes the gain of the resonant frequency point to decrease, resulting in an increase in system error. With the increase of the repetitive control gain factor K_{rc}, the gain of the repetitive controller at each frequency point will increase, making the system still have enough gain when the internal model factor Q is smaller. Therefore, the repetitive controller can have both high resonance gain and resonance bandwidth by reasonably selecting the internal mode coefficient Q and the gain coefficient K_{rc}.

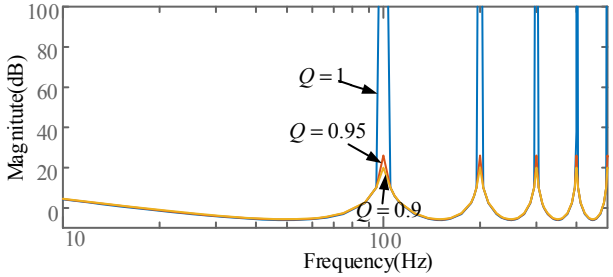

Fig.5. Repetitive controller with different internal model factor

C. Harmonic suppression based on repetitive controller

In this paper, a compound regulator in parallel with PI and repetitive controllers in the *d-q* coordinate system is used. The structure diagram of *d* axis shown in Fig. 5, *q* axis is similar to that. The preceding analysis shows that the 5, 7, 11 and 13 harmonics caused by the nonlinearity of general inverter and the back EMF of electric motor can be regarded as the 6 and 12 harmonics in the *d-q* coordinate system. Therefore, by setting the harmonic number as an integer multiple of the repetitive control frequency, we can suppress the harmonic of these specific frequencies by using the characteristic of the infinity gain and zero phase difference at the integer frequency multiplication point of the repetitive controller.

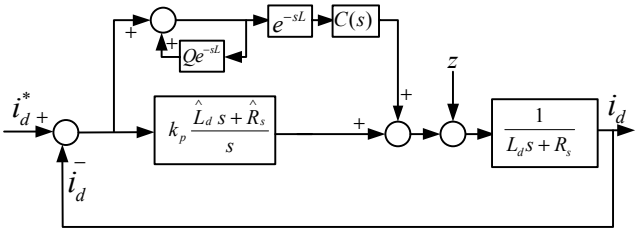

Fig.6. Diagram of current harmonic suppression based on repetitive control

In Fig. 6, the 5th and 7th harmonic current caused by factors such as inverter nonlinearity and back EMF nonlinearity are regarded as periodic perturbation input z, k_p is proportional coefficient of PI controller, and the superscript symbolic representation of the estimate. Besides, the PI regulator is configured to counteract the poles of the motor, is tuned to a fast, flexible I-type system. Where L is the repetitive controller cycle and *C(s)* is the compensator of the repetitive control loop.

For the composite regulator, discrete controller can be obtained in the form of $G_{\mathrm{Re}p}(z)=\dfrac{z^{-N}C(z)}{1-Q(z)z^{-N}}$, where $G_{PI}(z)$ is PI regulator, $r(z)$,$y(z)$ are input and output, $d(z)$ is disturbance, $G_P(z)$ is discrete motor model. Then the compound controller control system output and input and disturbance of the relationship is as follows.

$$y(z)=\frac{G_P(z)[G_{PI}(z)+G_{\mathrm{Re}p}(z)]}{1+G_P(z)[G_{PI}(z)+G_{\mathrm{Re}p}(z)]}r(z)+\frac{1}{1+G_P(z)[G_{PI}(z)+G_{\mathrm{Re}p}(z)]}d(z) \tag{18}$$

According to the theory of control theory, in order to make the system stable, the red line condition is that the closed-loop transfer function pole is located in the unit circle. The closed-loop system's characteristic equation is

$$1+G_P(z)[G_{PI}(z)+G_{\mathrm{Re}p}(z)]=0 \tag{19}$$

With the expression of the repetitive controller into the characteristic equation, (20) can be obtained.

$$0=[1-z^{-N}Q(z)][1+G_{PI}(z)G_P(z)]+z^{-N}C(z)G_P(z)= [1+G_{PI}(z)G_P(z)]\{1-z^{-N}[Q(z)-C(z)\frac{G_P(z)}{1+G_{PI}(z)G_P(z)}]\} \tag{20}$$

It can be expressed as (21), (22) respectively.

$$\Delta_1=[1+G_{PI}(z)G_P(z)] \tag{21}$$

$$\Delta_2=1-z^{-N}[Q(z)-C(z)\frac{G_P(z)}{1+G_{PI}(Z)G_P(z)}] \tag{22}$$

According to [18], we can conclude that the transfer function of the control object of the repetitive controller in the closed-loop system is as follows.

$$G_O(z)=\frac{G_P(z)}{1+G_{PI}(Z)G_P(z)} \tag{23}$$

Therefore, in order to stabilize the closed-loop system, only need to have the characteristic roots of A and B within the unit circle. According to [21] and [22], we can find that if we want to satisfy the characteristic roots in the unit circle, we need to meet the following two requirements: 1) the system is stable when the PI current loop regulator is adopted alone; 2) the conditions to add repetitive controller should be met (24) as follows.

$$\left|Q(z)-C(z)\frac{G_P(z)}{1+G_{PI}(Z)G_P(z)}\right|<1 \tag{24}$$

IV. Simulation Results

In order to verify the effectiveness of the harmonic suppression algorithm, this paper builds a simulation model under Matlab/Simlink and carries out a simulation analysis. The harmonic current in the simulation model is mainly introduced from two aspects of the air-gap magnetic field distortion and the nonlinearity of the inverter. On the one hand, considering the harmonic current introduced by the low-order harmonic back EMF of the PMSM in the simulation model and establishes the model of the permanent magnet synchronous motor with the back-EMF by the fifth and seventh harmonic flux linkage. On the other hand, the harmonic current is generated by adding 3 μs dead time in the inverter model. In the simulation model, the parameters of the PMSM drive system are shown in Table I.

TABLE I. Parameters of PMSM Drive System

Parameters	Description	Values
Stator resistance	R/Ω	0.5
d-axis inductance	L_d /mH	6
q-axis inductance	L_q/ mH	6
Number of pole pares	p_n	4
Mechanical inertia	J/(kg·m^2)	0.001
Fundamental flux linkage	ψ_{f1} /Wb	0.2
5 harmonic flux linkage	ψ_{f5} /Wb	0.01
7 harmonic flux linkage	ψ_{f7} /Wb	0.006
DC bus voltage	u_{dc}/V	300
Switching frequency	kHz	10
Dead time	μs	3

Fig. 7 and Fig. 8 show the comparison of the simulated waveforms before and after adding the harmonic suppression module when the permanent magnet synchronous motor is operating at a given rotation speed of 1500 r/min. The frequency of the fundamental current of the motor is 100Hz.

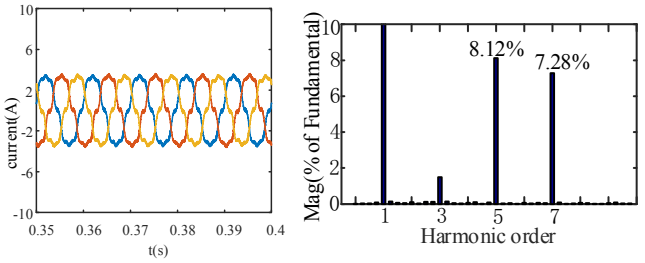

(a) current waveform (b) harmonic analysis

Fig.7. Current waveform and harmonic analysis without suppression

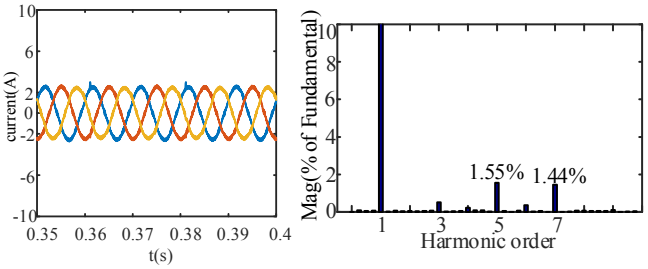

(a) current waveform (b) harmonic analysis

Fig.8. Current waveform and harmonic analysis with suppression

Fig. 7 (a) shows that before the repeating controller was added, the three-phase current was distorted due to the dead time of 3 s and distortion of the air gap magnetic field of the motor body. By Fourier analysis, it can be found that the main 5, 7 harmonic current, which is consistent with the previous analysis of the theory of harmonic sources. Fig. 8 (a) shows that after adding a harmonic suppression algorithm containing the repetitive controller, the three-phase current has a significant improvement, and the waveform is basically a standard sine wave. After the fast Fourier transform analysis of the A phase current, the waveforms shown in Fig. 7 (b) and 8 (b) are obtained. Compared with the two diagram, it can be found that after adding repetitive controller, the 5th and 7th harmonic contents in motor current decreased from 8.12% and 7.28% to 1.55% and 1.44%, respectively. The total harmonic distortion rate of current harmonic decreased from 11.39% to 4.25%. From the simulation results, it can be seen that the compound regulator with repetitive controller can achieve a good effect on the suppression of the 5 times and 7 times harmonic currents.

V. Experimental Results

Experimental is carried out on the PMSM experimental platform to verify the effectiveness of the proposed method of Harmonic current suppression algorithm based on repetition controller. Fig. 9 and Fig. 10 are the current waveforms and their harmonic analysis before and after using the proposed algorithm. As shown in Fig. 9 and Fig. 10, it can be found that after adding repetitive controller, the 5th and 7th harmonic contents in motor current decreased from 12.48% and 8.85% to 3.45% and 2.42%, respectively. From the experimental results, it can be seen that the proposed repetition controller based harmonic suppression algorithm can effectively reduce current harmonics of the permanent magnet synchronous motor.

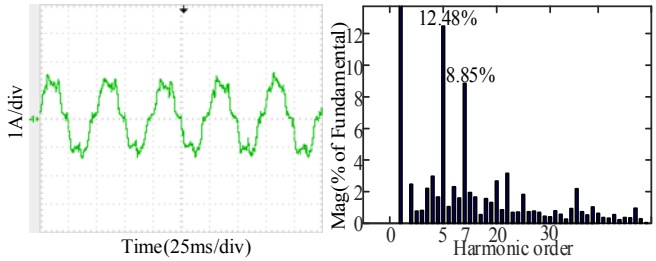

(a) current waveform (b) harmonic analysis

Fig.9. Current waveform and harmonic analysis without suppression

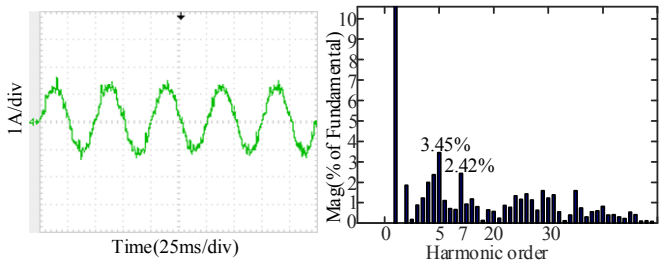

(a) current waveform (b) harmonic analysis

Fig.9. Current waveform and harmonic analysis with suppression

VI. Conclusions

In this paper, aiming at the problem of high current harmonic content in the running process of PMSM, a compound current regulator with parallel repetitive controller in current PI regulator is proposed to suppress the harmonic current of PMSM. This paper deduces the mathematical relationship between repetitive controller with internal coefficient Q and PR controller. Simulation results and expermental results show that this algorithm can effectively suppress the 5th and the 7th harmonic current, and improve the sine degree of the motor current.

References

[1] Q. Wei, and T.A. Nondhal, "Mutual Torque Ripple Suppression of Surface-mounted Permanent Magnet Synchronous Motor," Eighth International Conference on Electrical Machines and Systems. IEEE, 2005, pp. 315-320 .

[2] S.H. Han, T.M. Jahns, and Z.Q. Zhu, "Analysis of Rotor Core Eddy-Current Losses in Interior Permanent Magnet Synchronous Machines," IEEE Transactions on Industry Applications, 2010, Vol. 46, No. 1, pp. 196-205.

[3] A.C. Oliveira, C.B. Jacobina, and A.M.N. Lima, "Improved Dead-Time Compensation for Sinusoidal PWM Inverters Operating at High Switching Frequencies," IEEE Transactions on Industrial Electronics, 2007, Vol. 54, No. 4, pp. 2295-2304.

[4] B. Chen, G. Liu, and K. Mao, "Harmonic current suppression for high-speed permanent magnet synchronous motor with sensorless control," International Conference on Electrical Machines and Systems. IEEE, 2017.

[5] J. Gao, X. Wu, and S. Huang, et al, "Torque ripple minimisation of permanent magnet synchronous motor using a new proportional resonant controller," Iet Power Electronics, 2017, Vol. 10, No. 2, pp. 208-214.

[6] D.G. Holmes, B.P. Mcgrath, and S.G. Parker , "Current Regulation Strategies for Vector-Controlled Induction Motor Drives," IEEE

Transactions on Industrial Electronics, 2012, Vol. 59, No. 10, pp. 3680-3689.

[7] Y.K. Lin, and Y.S. Lai, "Dead-time elimination of PWM-controlled inverter/converter without separate power sources for current polarity detection circuit," IEEE Transactions on Industrial Electronics, 2009, Vol. 56, No. 6, pp. 2121-2127.

[8] R.J. Kerkman, D.Leggate, and D.W. Schlegel, et al, "Effects of parasitics on the control of voltage source inverters," IEEE Transactions on Power Electronics, 2003, Vol. 18, No. 1, pp. 140-150.

[9] S.Y. Kim, W. Lee, and M.S. Rho, et al, "Effective Dead-Time Compensation Using a Simple Vectorial Disturbance Estimator in PMSM Drives," IEEE Transactions on Industrial Electronics, 2010, Vol. 57, No. 5, pp. 1609-1614.

[10] Z. Tang, and B. Akin, "Compensation of dead-time effects based on revised repetitive controller for PMSM drives," Applied Power Electronics Conference and Exposition, IEEE, 2017, pp.2730-2737.

[11] L. Schwager, A. Tüysüz, and C. Zwyssig, et al, "Modeling and comparison of machine and converter losses for PWM and PAM in high-speed drives," International Conference on Electrical Machines, IEEE, 2012, pp. 995-1006.

[12] N. Urasaki, T. Senjyu, and K. Uezato, et al, "Adaptive Dead-Time Compensation Strategy for Permanent Magnet Synchronous Motor Drive," IEEE Transactions on Energy Conversion, 2007, Vol. 22, No. 2, pp. 271-280.